INFECTION AND IMMUNITY, May 2006, p. 2587–2595 Vol. 74, No. 5
0019-9567/06/$08.00+0 doi:10.1128/IAI.74.5.2587–2595.2006

OspE2 of *Shigella sonnei* Is Required for the Maintenance of Cell Architecture of Bacterium-Infected Cells

Masashi Miura,[1,2] Jun Terajima,[1] Hidemasa Izumiya,[1] Jiro Mitobe,[1] Teruya Komano,[2] and Haruo Watanabe[1]*

Department of Bacteriology, National Institute of Infectious Diseases, Shinjuku, Tokyo, Japan,[1] *and Department of Biology, Tokyo Metropolitan University, Hachioji, Tokyo, Japan*[2]

Received 31 August 2005/Returned for modification 24 October 2005/Accepted 7 February 2006

The OspE2 product of *Shigella* spp., the expression of which is regulated by the *mxiE* gene, is secreted through a type III secretion system into host cells. We investigated the function of OspE2 of *Shigella sonnei* by using cultured epithelial cells. Cells invaded by an *ospE2* deletion mutant altered their morphology into the rounding shape, which was not due to cell death, whereas cells invaded by the wild-type strain kept their cell shape intact. The *ospE2* mutation did not affect initial cell entry and multiplication in cells, but the mutant formed smaller-than-normal plaques on cell monolayers, indicating a deficiency in cell-to-cell spread by the bacteria. An *mxiE* deletion mutant also showed changes in cell morphology and deficiency in bacterial spread to adjacent cells. In cells invaded by the *ospE2* mutant, disturbance of actin stress fibers was prominent at 3 h after invasion. Analysis of OspE2 localization indicated that the OspE2 protein accumulated on focal contact-like structures in the infected host cells. These results suggest that colocalization of the OspE2 protein in the focal contacts of infected cells may function to maintain an intact cell morphology. The morphological change induced by invasion of the *ospE2* mutant may affect secondary bacterial transmission.

Shigella spp., which are able to invade epithelial cells, are the causative agents of bacillary dysentery in humans (21). A large, 230-kb virulence plasmid in virulent *Shigella* is involved in invasion (43, 56). After internalization, *Shigella* strains lyse the phagocytic vacuole and enter the cell cytosol, where they multiply and move to invade adjacent cells (10, 43, 44). An outer membrane protein, VirG (IcsA), encoded on the virulence plasmid is involved in intra- and intercellular movements, which it accomplishes by polymerizing an actin tail that propels the bacterium through the cytoplasm and into adjacent cells (3, 24, 25). In this process, the moving bacterium forms protrusions from the cytoplasmic membrane as it enters adjacent cells (3, 17, 36, 40). During reinfection, bacteria reside within two membranes that belong to the protrusion and to the newly infected cell and subsequently lyse these two membranes by using IcsB (1), which is also involved in the escape of intracellular *Shigella* cells from autophagy (33).

The large virulence plasmid of *Shigella* contains the *mxi-spa* and *ipa* gene cluster, termed the "31-kb entry region" (for a review, see reference 39). *mxi-spa* comprises about 20 genes mostly coding for a type III secretion (TTS) apparatus, which is a bacterial multiprotein complex that forms a needle-like structure (45, 48). The *ipa* operon encodes effector proteins such as IpaB, IpaC, and IpaD. These proteins are translocated into the intracellular milieu of the host cells through the apparatus and act on various components of cytoskeletal architecture or eukaryotic signal transduction pathways to modulate host cell function (7, 51, 59).

Secretion of effector proteins from *Shigella* cells is induced by their contact with host cells (29) or by addition of the dye Congo red to the growth medium (2, 38). Inactivation of *ipaB* or *ipaD* gives rise to constitutive secretion of effector proteins (38). Under these conditions, 14 other TTS apparatus-secreted proteins were identified in *Shigella flexneri*, including the Osp proteins (for "outer *Shigella*") OspB, OspC1 to OspC4, OspD1 to OspD3, OspE1 and OspE2, OspF, and OspG (6). Genes for these proteins are mainly located outside the 31-kb entry region in the virulence plasmid (6, 9) and are regulated by MxiE, an activator protein of the AraC family, which is encoded within the *mxi-spa* operon and requires IpgC as a coactivator (18, 26). Most of the promoters for *osp* genes contain a 17-bp motif, the MxiE box, which is essential for activation of these promoters by MxiE (27). The *mxiE* mutant is invasive to cultured cells but completely avirulent in in vivo animal models (18). Hence, the functions of genes regulated by MxiE are thought to be essential for later steps in infection. The *virA*, $ipaH_{1.4}$, $ipaH_{2.5}$, $ipaH_{4.5}$, $ipaH_{7.8}$, and $ipaH_{9.8}$ genes have also been found to be regulated by MxiE (23). The functions of some of the MxiE-regulated genes have been revealed. For example, OspG negatively controls innate immune responses by targeting ubiquitin-conjugating enzymes (20). $IpaH_{9.8}$ is transported to the nucleus of mammalian cells and binds to a splicing factor, U2AF (35), to modulate immune responses of the host cells (34, 50). $IpaH_{7.8}$ promotes the escape of *Shigella* cells from vacuoles of macrophages (10). VirA is capable of interacting with tubulin to promote microtubule destabilization and bacterial internalization (53, 58). The secreted anti-activator OspD1 and coantiactivator Spa15 are involved in the control of transcription by MxiE-IpgC (37). However, the functions of the other MxiE-regulated genes remain to be elucidated.

In this study, we focused on the function of the *ospE2* gene, which is one of the MxiE-regulated genes. We have demon-

* Corresponding author. Mailing address: Department of Bacteriology, National Institute of Infectious Diseases, Toyama 1-23-1, Shinjuku, Tokyo 162-8640, Japan. Phone: 81-3-5285-1337. Fax: 81-3-5285-1193. E-mail: haruwata@nih.go.jp.

TABLE 1. Bacterial strains and plasmids used in this study

Strain or plasmid	Genotype or description	Source or reference
S. sonnei strains		
HW383	*S. sonnei* wild-type strain; Tet^r	55
HW506	Virulence plasmid-cured HW383	55
MS390	HW383 antibiotic-sensitive strain; Tet^s	30
MS1303	MS390 Δ*ospE2*	This study
MS1307	MS390 Δ*mxiE*	This study
MS1330	MS390 Δ*ospE2* Δ*spa40*	This study
Plasmids		
pHW1273	Amp^r derivative of a large virulence plasmid, pSS120, of *S. sonnei* HW383	19
pHW745	pHSG595 (pSC101 replicon) derivative carrying *virF*; Cm^r	54
pF3	pHW745 derivative carrying a 5-kb Sau3AI fragment of *ospE2*; Cm^r	This study
pKD46	λ *red* helper plasmid; Amp^r	8
pKD13	Template plasmid with Km resistance gene and FLP recognition target	8
pCP20	FLP helper plasmid; Cm^r	8
pUC19	Multicopy cloning vector; Amp^r	57
pET-28a	Expression vector for recombinant protein with His fusion tag and T7 promoter; Km^r	47
pTH18cr	pSC101 replicon cloning vector; Cm^r	13
pK19	Multicopy cloning vector; Km^r	41
pIRES-hrGFP-2a	Expression vector for recombinant protein with HA fusion tag; Amp^r	Stratagene
pIRES-Cm	pIRES-hrGFP-2a derivative; Amp^r Cm^r	This study
pMM102	pUC19 derivative carrying an entire *ospE2* gene with the *ospE2* promoter	This study
pMM500	pTH18cr derivative carrying the *ospE2* gene with the *lacZ* promoter	This study
MM700	pET28a derivative carrying the *ospE2* gene	This study
pMM800	pIRES-hrGFP-2a derivative carrying *ospE2* gene with HA tag; Amp^r	This study
pMM800Cm	pIRES-hrGFP-2a derivative carrying *ospE2* gene with HA tag; Amp^r and Cm^r	This study
pMM819K	pK19 derivative carrying the *ospE2*-HA gene with the *lacZ* promoter	This study

strated that both an *ospE2* deletion mutant and an *mxiE* deletion mutant caused morphological change in bacterially infected cells. OspE2 protein was secreted in a TTS system (TTSS)-dependent manner and was located in the focal contact-like structures of infected host cells. We discuss a role of OspE2 in maintenance of host cell morphology.

MATERIALS AND METHODS

Bacterial strains, plasmids, cell culture, and media. The bacterial strains and plasmids used in this study are listed in Table 1. HeLa cells and HEp2 cells were grown in minimal essential medium (MEM) with 10% fetal calf serum (FCS) in a 5% CO_2 incubator. Bacterial cells were grown in LB broth or on LB plates containing 1.5% Bacto agar. Antibiotic concentrations were as follows: chloramphenicol (Cm), 25 μg/ml; ampicillin (Amp), 100 μg/ml; kanamycin (Km), 50 μg/ml.

Cloning of the *ospE2* gene. For cloning of the *Shigella sonnei ospE1* and *ospE2* genes, shotgun cloning of pHW1273 DNA was performed. DNA resulting from a partial digestion of pHW1273 with Sau3AI was fractionated by agarose gel electrophoresis, and fragments (5 to 10 kb) were ligated into the BamHI site of pHW745. The ligation mixture was used for electroporation. The transformants were colony hybridized with an *ospE2* gene probe of *S. flexneri* under conditions of low stringency, and positive colonies were sequenced. The clone pF3, carrying the *ospE2* gene, was selected. The clone of *ospE1* was isolated in a similar way.

Construction of deletion mutants. The *ospE2* deletion mutant in *S. sonnei* was constructed by the PCR-based gene disruption method (8, 30). MS390 harboring the λ red helper plasmid pKD46 was used for construction of the mutant. The plasmid pKD13 was used as a template for PCR using primers appropriate to amplify a Km^r marker flanked by *ospE2*-specific sequences. After replacement of the target gene by the Km^r marker, flipase (FLP)-mediated recombination was performed to remove the resistance marker. The deletion mutation was confirmed by Southern analysis and DNA sequencing. The construction of *S. sonnei mxiE* and *spa40* mutant strains was performed in a similar way.

Construction of plasmids encoding OspE2. For subcloning of the *ospE2* gene, a 744-bp DNA fragment resulting from partial digestion of pF3 with Sau3AI was ligated with BamHI-digested pUC19 in the orientation opposite the *lac* promoter, yielding pMM102. Plasmids pMM500, pMM700, and pMM800 were constructed as follows: the *ospE2* gene was amplified by PCR with *TaKaRa Ex Taq* DNA polymerase (Takara Bio Inc.) and pMM102 DNA as a template, using a forward primer containing an EcoRI site and a reverse primer containing a PstI site for construction of pMM500, a forward primer containing an NdeI site and a reverse primer containing an EcoRI site for construction of pMM700, and a forward primer containing an EcoRI site and a reverse primer containing a SalI site for construction of pMM800. The PCR products were digested with the appropriate restriction enzymes and cloned into pTH18cr, pET-28a, or pIRES-hrGFP-2a, resulting in pMM500, pMM700, or pMM800, respectively. The plasmids pMM800 and pIRES-hrGFP-2a were inserted by Cm^r gene exchange (Exchanger System; Stratagene) using the *loxP* site on the vector and Cre recombinase in vitro, resulting in pMM800Cm and pIRES-Cm, respectively. For construction of pMM819K, the *ospE2* gene with a hemagglutinin (HA) tag (*ospE2*-HA) was amplified by PCR with pMM800 DNA as a template, using a forward primer containing a PstI site and a reverse primer containing an EcoRI site, and was cloned into pK19. The structure of each construct was confirmed by DNA sequencing and restriction enzyme analysis.

Sodium dodecyl sulfate-polyacrylamide gel electrophoresis (SDS-PAGE) and immunoblotting. Electrophoresis of proteins on polyacrylamide gels in the presence of SDS was performed as described by Laemmli (22) with slight modifications. Immunoblotting analyses were carried out with convalescent-phase serum of an *S. flexneri*-infected monkey (54) and rabbit anti-VirG antiserum, which was obtained by immunization of rabbits with a synthesized peptide (unpublished data). For the preparation of rabbit anti-OspE2 antiserum, rabbits were immunized with His-tagged OspE2, which was purified from *Escherichia coli* BL21 harboring pMM700. The monospecific rabbit polyclonal anti-IpaC antibody used for immunoblotting was described previously (46). Anti-rabbit immunoglobulin G conjugated to horseradish peroxidase was obtained from Jackson Laboratories. Immunoblot detection was carried out with the ECL kit (Amersham).

Plaque assay. The intra- and intercellular dissemination of bacteria was evaluated with the plaque formation assay (32). HEp2 cells were seeded onto six-well plates and grown for 2 days to confluent monolayers. Bacteria were inoculated into the cells at a multiplicity of infection of 30, and the cells were incubated for 2 h at 37°C. After three washes with phosphate-buffered saline (PBS), MEM containing 5% FCS and 100 μg/ml of gentamicin was added, and the cells were grown for 2 or 4 days at 37°C in the presence of CO_2. After Giemsa staining, plaque diameters were measured.

Invasion assay. Bacterial invasion of HeLa or HEp2 cells was tested with the gentamicin protection assay (49). HeLa or HEp2 cells were grown on six-well tissue culture plates to semiconfluent monolayers in MEM with 10% FCS in a

5% CO_2 incubator. Cells were infected with bacteria grown to log phase in LB at 37°C at a multiplicity of infection of 100, centrifuged at 900 × *g* for 5 min at 37°C, and further incubated at 37°C for 20 min. Cells were washed three times with PBS, and gentamicin was added to the medium at a final concentration of 200 μg/ml, followed by further incubation at 37°C for 20 min (19). For the invasion assay, the cells were lysed in 1 ml of PBS containing 0.1% Triton X-100 per well, and the number of bacteria invaded was counted after plating onto LB agar. For intracellular growth, cells were further incubated for 20 or 290 min and then lysed in 1 ml of PBS containing 0.1% Triton X-100 per well. After incubation at room temperature for 10 min, the lysates containing bacterial cells were diluted and plated onto LB agar plates in triplicate. Colonies grown on LB plates were counted. Assays were repeated three times. The results of the assays were expressed as the percentage of the number of surviving bacteria relative to that of bacteria initially added to the cell culture.

For estimating the frequency of host cell rounding, cells having more than five bacteria after Giemsa staining were grouped by the following criteria: nonspreading host cells were defined as rounded cells, and spreading cells with normal morphology were defined as nonrounded cells. The percentage of bacterium-invaded cells adopting rounded morphology was determined by counting at least 300 infected cells from three randomly selected light microscopy fields in each of three independent wells (>80 cells/field).

Analysis of secreted proteins. For assays of Ipa and OspE2 production and secretion, bacterial cells were grown at 37°C in LB to log phase. After centrifugation at 14,000 × *g* for 2 min, the bacterial pellet was resuspended in 3 ml of PBS. Congo red was added to a bacterial suspension at a final concentration of 0.002%, and the suspension was further incubated at 37°C for 10 min. The sample was centrifuged at 14,000 × *g* for 2 min to give the bacterial pellet and supernatant fraction. The bacterial pellet was solubilized in SDS-PAGE sample buffer, boiled for 5 min, and subjected to SDS-PAGE. The supernatant was passed through a 0.45-μm-pore-size membrane filter, and proteins were precipitated with 6% trichloroacetic acid. The precipitates were washed with acetone and solubilized in SDS sample buffer, boiled for 5 min, and subjected to SDS-PAGE.

Immunofluorescence microscopy. HeLa or HEp2 cells grown on coverslips were infected with the indicated bacterial strains for 3 or 3.5 h on a six-well plate. The cells were washed, fixed with 3.7% paraformaldehyde in PBS for 20 min, and treated for 5 min with 50 mM NH_4Cl in PBS. Cells were rendered permeable to the antibody reagent with 0.1% Triton X-100 in PBS overnight at 4°C and treated with 1% bovine serum albumin in PBS for 1 h. To visualize F-actin, focal adhesion kinase (FAK), talin, or HA-tagged OspE2, permeabilized cells were labeled with 1/100-diluted Alexa 488-labeled phalloidin (Molecular Probes Inc.), 1/400-diluted rabbit anti-FAK antibody (Santa Cruz Biotechnology), 1/400-diluted rabbit anti-talin antibody (Santa Cruz Biotechnology), or 1/400-diluted mouse monoclonal antibody to HA (Sigma), respectively. For staining of bacterial cells, 1/100-diluted monospecific rabbit polyclonal anti-IpaC antibody (45) or 1/100-diluted rabbit anti-form I serum (Denka Seiken) was used. Cells were washed three times in PBS containing 0.1% Triton X-100 and treated with a 1/400 dilution of fluorescein isothiocyanate-conjugated goat anti-mouse immunoglobulin antibody (Molecular Probes Inc.), Texas Red-conjugated sheep anti-rabbit immunoglobulin antibody (Molecular Probes Inc.), or Texas Red-conjugated sheep anti-mouse immunoglobulin antibody (Molecular Probes Inc.). Cells were washed three times in PBS containing 0.1% Triton X-100, washed twice in PBS, and then mounted. Samples were analyzed by fluorescence microscopy using an Olympus BX51 microscope equipped with a 40× lens objective. Images were captured with an Olympus E-20 digital camera and processed with Adobe Photoshop 5.5.

Assays for cell death. For extraction of cellular DNA and gel electrophoresis, HeLa cells (3.6×10^6) infected with the indicated strains or treated with 30 ng/ml tumor necrosis factor alpha (TNF-α) (Wako) plus 60 μg/ml cycloheximide (Sigma-Aldrich) for 3 h or 5 h were washed with PBS and lysed for 20 h at 37°C in lysis buffer (1% SDS, 100 mM NaCl, 10 mM Tris, 1 mM EDTA [pH 8.0]) supplemented with proteinase K (1 mg/ml). After three phenol and chloroform/isoamylalcohol (24:1) extractions, the DNA was precipitated with ethanol, dried, resolved in 10 mM Tris–1 mM EDTA (pH 8.0) supplemented with 1 μg/ml RNase A, separated on a 1.5% agarose gel, and visualized by ethidium bromide staining. Pictures were taken under UV light.

For terminal deoxynucleotidyltransferase-mediated dUTP-biotin nick end labeling (TUNEL), HeLa cells infected with the indicated strains or treated with 30 ng/ml TNF-α plus 60 μg/ml cycloheximide for 3 h or 5 h were washed with PBS, fixed, and permeabilized, and biotinylated nucleotide was incorporated enzymatically (TACS 2 TdT-Fluor In Situ Apoptosis Detection kit; Trevigen) into fragmented chromosomal DNAs, which were detected with a fluorescein conjugate of streptavidin. Nuclear fluorescence in HeLa cells was evaluated by fluorescence microscopy with the use of an Olympus BX51 microscope as described above.

Cytotoxicity was analyzed with the CytoTox 96 kit (Promega). The degree of cytotoxicity was evaluated by quantifying the amount of cytoplasmic lactate dehydrogenase (LDH) was released into supernatants from HeLa cells infected with the indicated strains or treated with 30 ng/ml TNF-α plus 60 μg/ml cycloheximide for 1, 3, or 5 h in 96-well plates. The percentage of cytotoxicity was determined by the following formula: [(released LDH activity − basal LDH activity in the supernatant)/(total LDH activity in the cells and supernatant − basal LDH activity in the supernatant)] × 100.

Nucleotide sequence accession numbers. The nucleotide sequences of *ospE1* and *ospE2* of *S. sonnei* were deposited in the DDBJ/EMBL/GenBank databases under accession numbers AB185406 and AB185407, respectively.

RESULTS

Construction and characterization of an *ospE2* deletion mutant of *S. sonnei*. While the *ospE* gene family, designated *ospE1* and *ospE2*, is known to be found in the *S. flexneri* large virulence plasmid (6), it is not known how many copies of *ospE* genes there are in the *S. sonnei* large virulence plasmid pHW1273. We first cloned *ospE2* of *S. sonnei* as described in Materials and Methods. Sequence analysis demonstrated that the *ospE2* gene of *S. sonnei* was 267 bp in length (88 amino acids), which was the same length as that of *S. flexneri* (6) but with 6 nucleotide substitutions, resulting in 5 amino acid substitutions in the C-terminal region of the product (A75V, D78V, Y85H, D87N, and F88I [*S. flexneri* versus *S. sonnei*]). The promoter region of the *S. sonnei ospE2* gene contains the MxiE box, which is essential for the activation by MxiE, suggesting that *ospE2* of *S. sonnei* is regulated by MxiE, as is the case in *S. flexneri* (27). *ospE2* of *S. sonnei* encodes a small protein of 10 kDa, which exhibits considerable similarities in amino acid sequence to ECs1567 and ECs1821 of enterohemorrhagic *E. coli* O157 (14), although their functions have not been revealed so far. Southern blotting experiments using an *S. sonnei ospE2* gene probe indicated that only one band was seen in pHW1273 under high stringency conditions, while two bands (*ospE1* and *ospE2*) were detected under low stringency conditions (data not shown). However, sequencing of the *ospE1* gene of pHW1273 indicated that *ospE1* is inactive in *S. sonnei*, since deduced translation of the *ospE1* gene stopped at the 14th codon, yielding a putative protein of 13 amino acids. Thus, only the *ospE2* gene was expected to be active in *S. sonnei*.

To characterize the role of *ospE2* in infection, we constructed a deletion mutant of the *ospE2* gene on the large virulence plasmid of *S. sonnei* MS390 by using the PCR-based gene disruption method (30). The *ospE2* mutant, designated MS1303, was used for cell assays. HEp2 cells of semiconfluent monolayers were infected with *S. sonnei* MS390 (wild type), MS1303 (Δ*ospE2*), and MS1303/pMM500 (Δ*ospE2*/*ospE2*$^+$) for 3 h. HEp2 cells infected with MS1303 (Δ*ospE2*) displayed a prominent morphological change, a rounded shape with a retracted plasma membrane in which no clear protrusions were observed (Fig. 1A). In contrast, host cells infected with MS390 (wild type) exhibited a spreading cell shape, which was similar to that of mock infection.

Since the rounded shape was also observed less frequently in host cells infected with wild-type bacteria, the frequency of host cell rounding was estimated (Fig. 1B). The number of rounded host cells infected with MS1303 (Δ*ospE2*) was greater

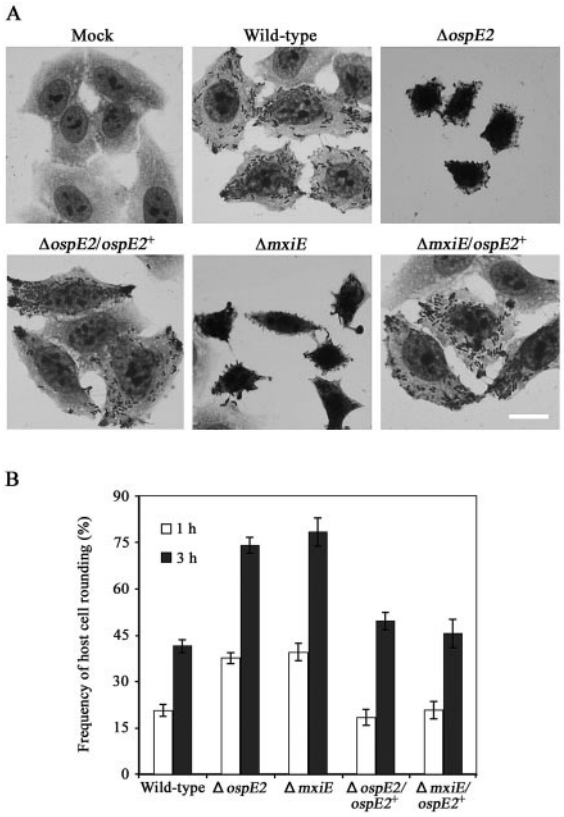

FIG. 1. Morphological changes in HEp2 cells after infection with *S. sonnei* Δ*ospE2* and Δ*mxiE* mutants. (A) HEp2 cells were infected with *S. sonnei* HW506 (mock), MS390 (wild type), MS1303 (Δ*ospE2*), MS1303/pMM500 (Δ*ospE2*/*ospE2*$^+$), MS1307 (Δ*mxiE*), or MS1307/pMM500 (Δ*mxiE*/*ospE2*$^+$). After 3 h, cells were fixed with methanol and stained with Giemsa reagent. Scale bar, 10 μm. (B) Frequency of host cell rounding (panel A) quantified. The frequency of rounding of mock-infected cells was less than 3% at both 1 and 3 h after infection. Error bars indicate standard deviations.

than that with MS390 (wild type) at both 1 and 3 h after infection. The frequency of host cell rounding of MS1303 (Δ*ospE2*) increased to nearly 80% by 3 h, whereas that of MS390 (wild type) remained almost half that of MS1303 (Δ*ospE2*) throughout the infection. Complementation of MS1303 (Δ*ospE2*) by pMM500 (*ospE2*$^+$) restored the frequency of morphological changes to the wild-type level. These results indicate that the *ospE2* gene is involved in the maintenance of host cell morphology.

We next examined the relationship between the morphological change caused by the *ospE2* mutation and virulence properties in the host cells (Table 2). The invasion efficiency of MS1303 (Δ*ospE2*) into HEp2 cells in semiconfluent monolayers was almost the same as that of MS390 (wild type) or MS1303/pMM500 (Δ*ospE2*/*ospE2*$^+$). MS1303 (Δ*ospE2*) produced and secreted Ipa proteins at levels similar to that of MS390 (wild type), suggesting that MS1303 (Δ*ospE2*) retains the same ability to invade host cells as the wild type. Intracellular multiplication of MS1303 (Δ*ospE2*) within 5.5 h after infection was also similar to that of MS390 (wild type). No distinct changes were noted in the VirG (IcsA) levels of *S. sonnei* MS390 (wild type) and MS1303 (Δ*ospE2*) (Table 2). These results indicate that the host cell rounding caused by the *ospE2* mutant and the *ospE2* mutation itself do not affect cell invasiveness and multiplication.

In gentamicin protection assays, the increase in the frequency of host cell rounding caused by the *ospE2* mutation during the course of infection suggests that the morphological changes are caused by intracellular, not extracellular, bacteria. However, a factor(s) in culture supernatants may be involved in the cell rounding. Thus, we performed experiments using bacterial culture supernatants of both the wild type and the *ospE2* mutant. However, no morphological changes in HEp2 cells were observed, even after 5.5 h of incubation with bacterial culture supernatants (data not shown). Therefore, we conclude that bacterial invasion is required for the changes into the rounded cell morphology.

Effects of the *S. sonnei mxiE* mutation on cell morphology similar to those of the *ospE2* mutation. Recently, Kane et al. (18) reported that transcription of *ospE2* in *S. flexneri* was activated by MxiE after infection and that the *mxiE* mutant showed a reduced plaque size phenotype. This led us to speculate that an *mxiE* mutant might have effects on infected cells similar to those of the *ospE2* mutant. In fact, HEp2 cells infected with MS1307 (Δ*mxiE*) displayed a rounded phenotype similar to that caused by the *ospE2* mutant (Fig. 1A and B). Furthermore, introduction of the *ospE2*$^+$ gene with the *lac* promoter (pMM500) in *trans* into MS1307 (Δ*mxiE*) completely rescued the morphology (Fig. 1A and B). The host cell rounding phenotype of the *ospE2* and *mxiE* mutants was also observed after infection of HeLa cells. These results suggest that *ospE2* and *mxiE* mutations affect host cell morphology simi-

TABLE 2. Characterization of *ospE2* mutants related to virulence in *S. sonnei*

Strain	Description	Invasion (%)[a]	Fold intracellular growth (5.5 h/1 h)[b]	Ipa production and secretion[c]	VirG (IcsA) expression[d]	Plaque size (mm)[e]
MS390	Wild type	0.32 ± 0.02	26.8 ± 2.5	+	+	0.8 ± 0.1
MS1303	Δ*ospE2*	0.33 ± 0.02	24.7 ± 2.9	+	+	0.3 ± 0.0
MS1303/pMM500	Δ*ospE2*/*ospE2*$^+$	0.35 ± 0.03	28.4 ± 2.1	+	ND	0.8 ± 0.1

[a] The number of bacteria recovered from gentamicin-treated cells at 40 min after infection was divided by the number of inoculated bacteria and then multiplied by 100. Values are means ± standard deviations from three independent wells.
[b] The number of bacteria recovered from gentamicin-treated cells at 5.5 h after infection was divided by the number of bacteria recovered from gentamicin-treated cells at 1 h after infection. Values are means ± standard deviations from three independent wells.
[c] Detection of IpaB and IpaC in PBS supernatants or whole-cell lysates after induction of secretion with Congo red by immunoblotting (see Materials and Methods).
[d] Detection of VirG (IcsA) in culture supernatants or whole-cell lysates by immunoblotting (see Materials and Methods). ND, not determined.
[e] Plaque diameters were measured at 96 h after infection. Values are means ± standard deviations for 50 plaques in each of three independent wells.

larly after infection and that the host rounding phenotype is dependent on OspE2 but independent of other effector proteins that are regulated by MxiE.

Host cell rounding without cell death. We next investigated the involvement of cell death in the morphological changes after infection with the *ospE2* mutant for 3 or 5 h. Fragmentation of cellular DNA into oligonucleosomes can occur in both types of cell death, apoptosis and necrosis (28, 35). Therefore, we tried to detect the chromosomal laddering in extracted DNA of MS1303 (Δ*ospE2*)-infected cells by gel electrophoresis and ethidium bromide staining (Fig. 2A). An apoptotic effect on HeLa cells is known to be achieved by treatment with TNF-α in combination with cycloheximide (31). The chromosomal DNA of HeLa cells treated with TNF-α plus cycloheximide was fragmented extensively into oligonucleosomes, clearly visible as a characteristic DNA ladder at 3 h after treatment (Fig. 2A, lane 2), whereas neither HeLa cells infected with MS1303 (Δ*ospE2*) and MS390 (wild type) nor HeLa cells untreated with TNF-α plus cycloheximide displayed fragmented DNAs (Fig. 2A, lanes 1, 3, and 4). Similar DNA patterns in each sample were also observed at 5 h after treatment or infection (data not shown).

Next, a TUNEL method was employed to check whether individual rounded cells infected with the *ospE2* mutant were free from fragmentation of host DNA (Fig. 2B). HeLa cells exhibiting morphological changes were stained by the TUNEL method at 3 h after treatment with TNF-α plus cycloheximide, whereas neither rounded HeLa cells infected with MS1303 (Δ*ospE2*) nor untreated cells showed any response (Fig. 2B). Similar staining patterns in each sample were also observed at 5 h after treatment or infection (data not shown).

To quantify the viability of rounded host cells infected with the *ospE2* mutant, we measured the activity of LDH released from the cells due to loss of host cell membrane integrity (Fig. 2C). HeLa cells treated with the drugs released about 40% and 70% LDH after 3 h and 5 h of incubation, respectively, whereas HeLa cells infected with MS390 (wild type) or MS1303 (Δ*ospE2*) for 5 h did not significantly release LDH. All of the above results suggest that rounded host cells infected with the *ospE2* mutant are viable at least within 5 h of infection and show no signs of apoptosis or necrosis.

Accumulation of OspE2 protein at focal contact-like structures in infected cells. To investigate how OspE2 affects host cell shape, we examined the localization of the OspE2-HA protein within infected host cells. *S. sonnei* OspE2 and OspE2-HA protein secretion via TTSS in vitro was confirmed by immunoblotting analysis; OspE2-HA was secreted in MS390 but not in the *spa40* mutant MS1330 (data not shown). HEp2 cells infected with *S. sonnei* strain MS1303/pMM819K (Δ*ospE2*/*ospE2*-HA$^+$) or MS1303/pK19 (Δ*ospE2*/− [i.e., the plasmid does not carry the *ospE2* gene]) for 3 h were processed for immunofluorescence microscopy using an anti-HA monoclonal antibody to reveal OspE2-HA (green signals) and anti-*S. sonnei* form I antibody to reveal bacterial cells (red signals), respectively (Fig. 3A). While HEp2 cells infected with MS1303/pK19 (Δ*ospE2*/−) changed to a rounded morphology, host cells infected with MS1303/pMM819K (Δ*ospE2*/*ospE2*-HA$^+$) restored the spreading morphology seen in uninfected HEp2 cells (the infected cells are indicated by red arrows in panels c and f in Fig. 3A), indicating that HA labeling of

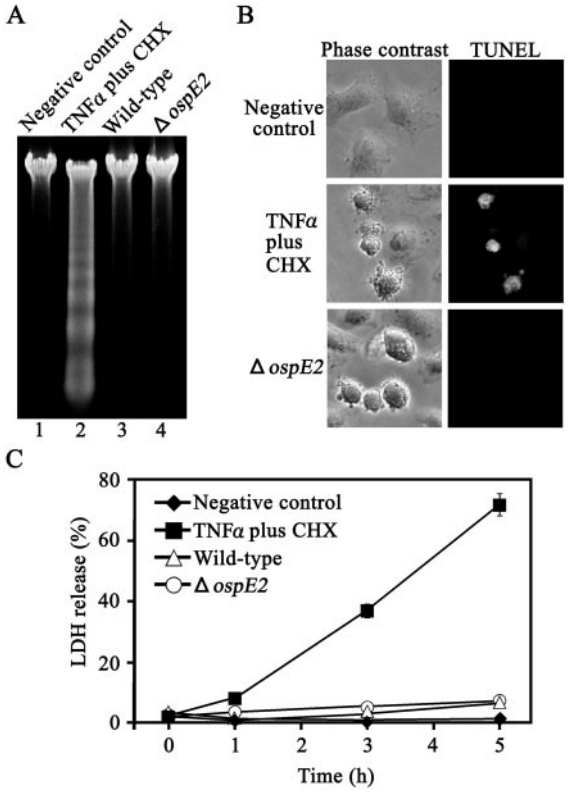

FIG. 2. Host cell rounding caused by the *S. sonnei* Δ*ospE2* mutant without cell death. (A) Absence of fragmentation of cellular DNA into oligonucleosomes after infection with the *S. sonnei* Δ*ospE2* mutant. DNA was extracted from 3.6×10^6 HeLa cells, separated on a 1.5% agarose gel, and visualized by ethidium bromide staining. Lane 1, no treatment (negative control); lane 2, treatment with 30 ng/ml TNF-α and 60 μg/ml cycloheximide (CHX) for 3 h to induce apoptosis (positive control); lane 3, infection with MS390 (wild type) for 3 h; lane 4, infection with MS1303 (Δ*ospE2*) for 3 h. (B) Host cell rounding caused by the *S. sonnei* Δ*ospE2* mutant without DNA fragmentation. HeLa cells were infected with *S. sonnei* MS1303 (Δ*ospE2*) for 3 h or treated with 30 ng/ml TNF-α plus 60 μg/ml CHX to induce apoptosis for 3 h (positive control). Untreated HeLa cells were used as a negative control. Cells were labeled by the TUNEL method, and reacted cells were detected by fluorescence microscopy. Phase-contrast and fluorescence pictures were taken of the same section. (C) Infection with the *S. sonnei* Δ*ospE2* mutant did not kill host cells. HeLa cells were infected with *S. sonnei* MS390 (wild type) or MS1303 (Δ*ospE2*) or treated with 30 ng/ml TNF-α plus 60 μg/ml CHX to induce apoptosis. Supernatants were taken at the indicated time points, and LDH released into the supernatants from host cells was assayed to measure cytotoxicity. The percentage of cytotoxicity was calculated as described in Materials and Methods. Each result represents the mean ± standard deviation from triplicate measurements.

OspE2 did not affect its activity. HEp2 cells infected with MS1303/pMM819K (Δ*ospE2*/*ospE2*-HA$^+$) showed numerous elongated green dots throughout the infected cell, while those without infection did not (white arrows in panel a in Fig. 3A). Some elongated dots were located at the cell periphery, where the bacteria were not colocalized (panel b). The elongated dot structures seemed to bear some resemblance to focal contacts (also known as focal adhesions or adhesion plaques) in their distribution and morphology. Such structures were not observed in mock-infected cells (data not shown). These results

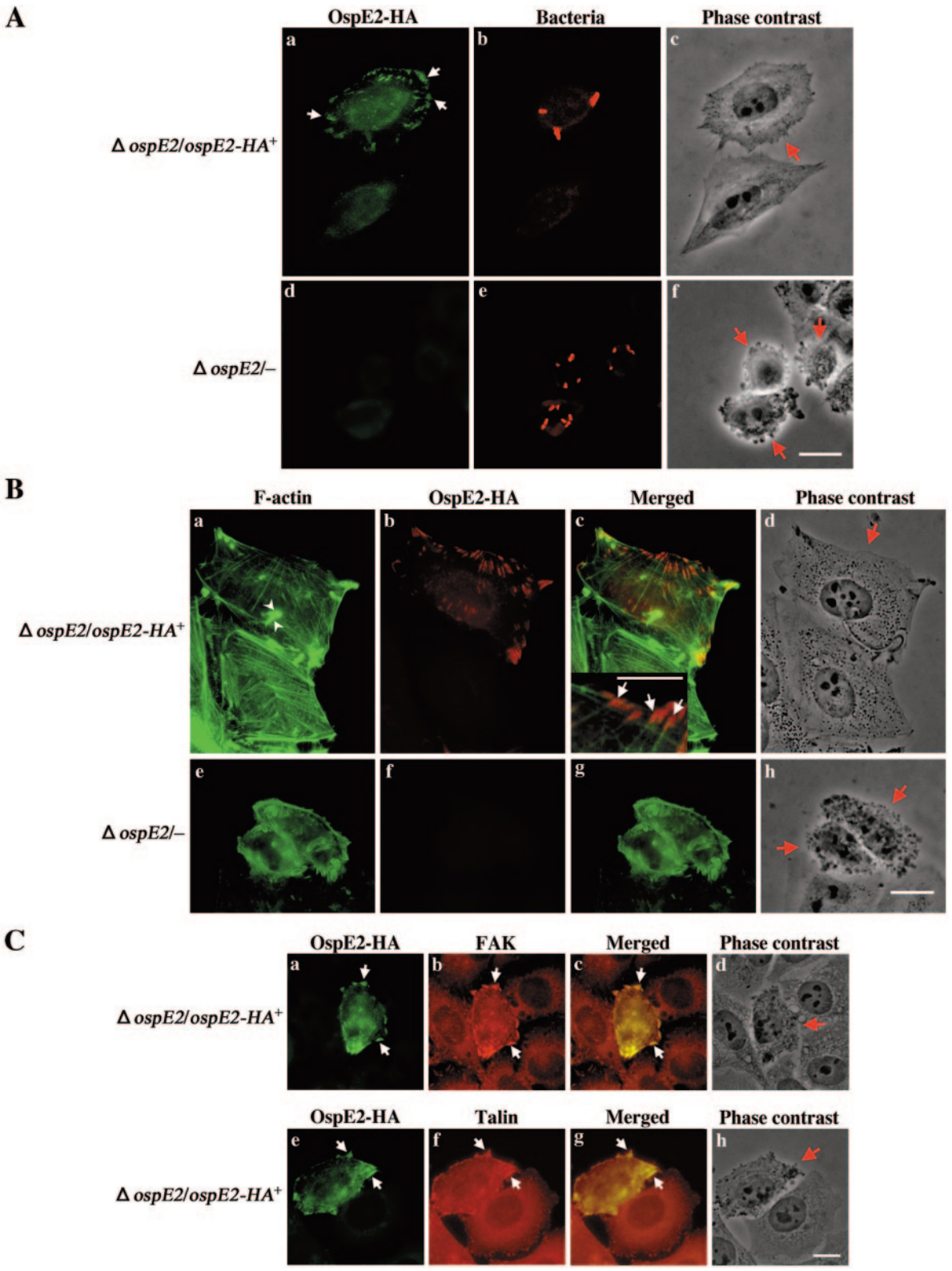

FIG. 3. OspE2-HA accumulates at focal contact-like structures in infected cells. (A) HEp2 cells were infected with *S. sonnei* MS1303/pMM819K (Δ*ospE2*/*ospE2*-HA$^+$) or MS1303/pK19 (Δ*ospE2*/−). After 3 h, the cells were fixed and immunostained. OspE2-HA was stained with anti-HA monoclonal antibody and secondary fluorescein isothiocyanate-tagged antibody. Bacterial cells were stained with anti-*S. sonnei* form I antibody and secondary Texas Red-tagged antibody. Single-color and phase-contrast images are shown for each strain. White arrows indicate the sites of accumulation of OspE2-HA signals. Red arrows in panels c and f indicate host cells with invaded bacteria. Scale bar, 10 μm. (B) HEp2 cells were infected with *S. sonnei* MS1303/pMM819K (Δ*ospE2*/*ospE2*-HA$^+$) or MS1303/pK19 (Δ*ospE2*/−) for 3 h and then subjected to

suggest that the OspE2 protein is secreted into the host cell cytosol after infection and accumulates at the focal contact-like structures.

To confirm that OspE2-HA accumulates at the focal contact-like structures of the host cells, we examined the spatial relationship between elongated dots of OspE2-HA and actin stress fibers, since actin stress fibers are known to terminate at the focal contacts (15). HEp2 cells infected with *S. sonnei* MS1303/pMM819K (Δ*ospE2*/*ospE2*-HA$^+$) or MS1303/pK19 (Δ*ospE2*/−) for 3 h were examined by immunofluorescence analysis using Alexa 488-conjugated phalloidin to visualize F-actin (green) and anti-HA antibody to visualize OspE2-HA (red) (Fig. 3B). The infected HEp2 cells are indicated by red arrows (panels d and h in Fig. 3B). Actin stress fibers were retained intact in the HEp2 cells infected with MS1303/pMM819K (Δ*ospE2*/*ospE2*-HA$^+$) but not in the cells infected with MS1303/pK19 (Δ*ospE2*/−) (panels a and e in Fig. 3B). HEp2 cells infected with MS1303/pMM819K (Δ*ospE2*/*ospE2*-HA$^+$) contained bacterial cells bearing actin comet tails (white arrowheads in panel a in Fig. 3B), which were not merged on localization of elongated dots of OspE2-HA (panel b in Fig. 3B). On the other hand, most of the visible actin stress fibers terminated at the sites where OspE2-HA accumulated (white arrows in the inset of panel c in Fig. 3B). These results suggest that the localization of elongated dots of OspE2-HA corresponds to that of focal contacts.

To ensure that the sites of OspE2-HA accumulation corresponded to the sites of protein complexes of focal contacts in the host cells, colocalization experiments by immunofluorescence microscopy using antibodies against FAK or talin, as indicators of focal contact proteins, were performed. HEp2 cells infected with MS1303/pMM819K (Δ*ospE2*/*ospE2*-HA$^+$) for 3 h exhibited signals for FAK or talin (both red) and OspE2-HA (green) (Fig. 3C). The infected HEp2 cells are indicated by red arrows in panels d and h (Fig. 3C). The focal contacts were observed in the infected host cells (white arrows in panels b and f in Fig. 3C), while in uninfected cells, small punctuated dots which were known as focal complexes and thought to be precursors of mature focal contacts were faintly observed at the cell periphery. The signals of OspE2-HA (green signals indicated by white arrows in panels a and e in Fig. 3C) were colocalized with the sites of these focal contacts in the infected cells (yellow signals in panels c and g in Fig. 3C). These results strongly suggest that OspE2 proteins accumulate at focal contact structures in the host cells.

Small plaque formation of the *ospE2* mutant. To test whether the *ospE2* mutant retains the ability of intra- or intercellular spread, plaque assays using confluent monolayers of HEp2 cells were performed. After HEp2 cells were infected with MS390 (wild type), MS1303 (Δ*ospE2*), and MS1303/pMM500 (Δ*ospE2*/*ospE2*$^+$), the sizes of plaques were measured (Table 2 and Fig. 4). MS1303 (Δ*ospE2*) produced smaller plaques than did MS390 (wild type). The diameter of the plaques developed by infection with MS1303 (Δ*ospE2*) was approximately 0.3 mm at 4 days after infection, while that of the plaques developed by MS390 (wild type) or MS1303/pMM500 (Δ*ospE2*/*ospE2*$^+$) was over 0.8 mm. These results suggest that the *ospE2* mutation affects the processes of secondary transmission of *Shigella* cells into neighboring host cells.

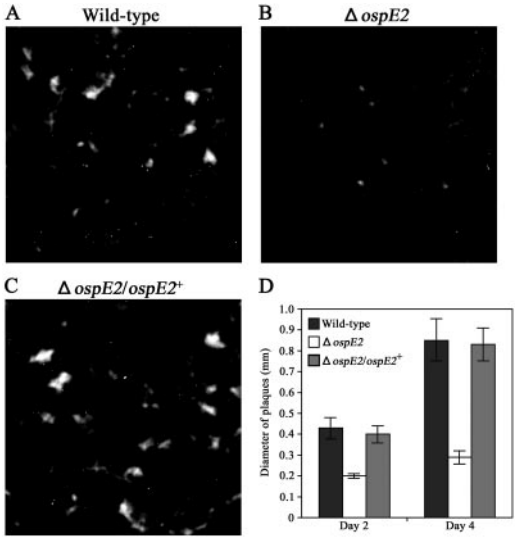

FIG. 4. Formation of small plaques in confluent monolayers of HEp2 cells after infection with the *S. sonnei* Δ*ospE2* mutant. Confluent monolayers of HEp2 cells were infected with *S. sonnei* MS390 (wild type) (A), MS1303 (Δ*ospE2*) (B), or MM1303/pMM500 (Δ*ospE2*/*ospE2*$^+$) (C) and incubated for 2 h. After a wash, medium containing gentamicin was added and culturing was continued at 37°C. At 4 days after infection, monolayers were stained with Giemsa to observe plaque formation by bacterial spreading. (D) Values in the bar graph represent mean ± standard deviation diameter for a total of 150 plaques from three independent wells.

DISCUSSION

The *ospE2* gene has been identified as one of the MxiE-regulated genes in *S. flexneri* (18, 23). Southern blotting analysis of the virulence plasmid indicated that *S. sonnei* also has two *ospE* genes, as is the case for *S. flexneri*. Sequence analysis of the *ospE1* gene of *S. sonnei* demonstrated that *ospE1* is a pseudogene. Hence, use of *S. sonnei* seemed to be more advantageous for functional analysis of *ospE2* gene. In this study, the role of the *S. sonnei ospE2* gene in infection was investigated. We found that the *ospE2* mutant causes morphological changes in infected cells and smaller plaque formation in cul-

immunofluorescence staining. F-actin was stained with Alexa 488-labeled phalloidin; OspE2-HA was stained with anti-HA monoclonal antibody and secondary Texas Red-tagged antibody. Single-color, merged, and phase-contrast images are shown. Actin stress fibers terminate at the site of OspE2-HA signals (white arrows in the inset of panel c). Red arrows in panels d and h indicate the infected cells. Scale bars represent 10 μm for panels d and h and 5 μm for the inset in panel c. (C) HEp2 cells infected with *S. sonnei* MS1303/pMM819K (Δ*ospE2*/*ospE2*-HA$^+$) for 3 h were stained with antibody against FAK (red) or talin (red) and OspE2-HA (green). Single-color, merged, and phase-contrast images are shown. White arrows indicate focal contact-like structures. Red arrows in panels d and h indicate infected cells. Scale bar, 10 μm.

tured epithelial cells, without effects on initial cell entry and multiplication in cells. Cultured supernatant of the *ospE2* mutant did not affect cell morphology. Only bacterium-invaded cells had the rounded phenotype, which was not due to the cell death. We also demonstrated that host cells infected with the *mxiE* mutant changed their morphology into the rounded shape, as host cells infected with the *ospE2* mutant did. This is another phenotypic similarity between *ospE2* and *mxiE* mutants, because the *mxiE* mutant is known to be deficient in plaque formation (18). For this reason, the morphological change of the host cells into rounding may correlate with the deficiency in plaque forming, namely, in the deficiency of secondary transmission of bacteria to adjacent cells. One explanation may be that the reduction of tight cell-to-cell contact caused by cell rounding affects the efficient spread of bacteria to adjacent cells.

Wild-type *S. sonnei* and the *ospE2*$^{+}$ complemented mutant did not cause the rounding phenotype of invaded cells; only the *ospE2* mutant did. This indicated that wild-type *Shigella* does not usually induce morphological changes even after invasion of the cells but that in the *ospE2* mutant, another factor(s) besides OspE2 seems to be involved in the induction of cellular morphological change. Since infection of HeLa cells with an *E. coli* K-12 strain carrying the *S. sonnei* 230-kb large virulence plasmid without the *ospE2* gene was sufficient to cause the cell rounding phenotype (data not shown), the large plasmid should contain the factors necessary for cell rounding. In the cells invaded by the *S. sonnei ospE2* mutant, the disturbance of protein complexes with FAK, talin, and actin stress fibers in the focal contact sites was prominent at 3 h after invasion (Fig. 3B and data not shown). This morphological change seems to be different from the membrane ruffling induced by the Ipa proteins of *Shigella* (51) or SopE of *Salmonella* (12) at the early stage of bacterial cell entry. Infection of *Yersinia pseudotuberculosis* is known to cause rounding of HeLa cells. YopH (4, 16), one of the effector proteins of *Yersinia*, which targets focal contacts of host cells and interacts with p130^{Cas}, is involved in cell rounding. *Yersinia* YopE, a GTPase-activating protein, induces disruption of the host cell-actin microfilament structure, allowing the bacterium to resist phagocytosis (5, 42). *S. sonnei* may have such factors for causing cell rounding, which should be elucidated in the near future.

A TTSS effector protein is mainly defined as the protein which is delivered into the cytoplasm of the host cell through the TTS apparatus. Accumulation of OspE2 to focal contact-like structures in infected host cells suggests that OspE2 acts as an effector protein. Because of the relatively low molecular size (approximately 10 kDa) of OspE2, it may be possible for OspE2 to diffuse throughout the cytoplasm of the cell immediately after bacterial invasion and to accumulate at the site of a putative target(s) near or at the focal contacts in order to fulfill its function. Therefore, the phenotype of the *ospE2* mutant to cause morphological change in host cells is more than coincidence, since some host cell proteins at the focal contacts are important determinants for the maintenance of cell morphology (52). This leads us to speculate that OspE2 protein colocalized in the focal contacts of infected cells may stimulate the function of focal contact proteins in order to keep the morphology of cells intact or to inhibit the above-described factor(s) which disturbs the focal contact-like structure. It is known that *Salmonella* SptP, which functions as a GTPase-activating protein of Rho-family GTPases, restores the change in cellular architecture (11). We did not find any similarity in nucleotide sequences between *ospE2* and other TTS effector protein-associated genes involved in the maintenance of cellular architecture.

We have described here the finding that OspE2 prevents the alteration of host cell shape at the postinvasion stage of infection. This remarkable adaptation to the modulation of host cell response may be advantageous for intracellular *Shigella* cells to disseminate into adjacent cells.

ACKNOWLEDGMENTS

We thank E. Arakawa, K. Hirose, and S. Iyoda for helpful advice and discussions. The cloning vectors pTH18cr and pK19 were gifts from the cloning vector collection of the National Institute of Genetics (Japan).

This work was supported by a grant from the Ministry of Education, Science and Technology.

REFERENCES

1. **Allaoui, A., J. Mounier, M. C. Prevost, P. J. Sansonetti, and C. Parsot.** 1992. *icsB*: a *Shigella flexneri* virulence gene necessary for the lysis of protrusions during intercellular spread. Mol. Microbiol. **12:**1605–1616.
2. **Bahrani, F. K., P. J. Sansonetti, and C. Parsot.** 1997. Secretion of Ipa proteins by *Shigella flexneri*: inducer molecules and kinetics of activation. Infect. Immun. **65:**4005–4010.
3. **Bernardini, M. L., J. Mounier, H. d'Hauteville, M. Coquis-Rondon, and P. J. Sansonetti.** 1989. Identification of *icsA*, a plasmid locus of *Shigella flexneri* that governs bacterial intra- and intercellular spread through interaction with F-actin. Proc. Natl. Acad. Sci. USA **86:**3867–3871.
4. **Black, D. S., and J. B. Bliska.** 1997. Identification of p130^{Cas} as a substrate of *Yersinia* YopH (Yop51), a bacterial protein tyrosine phosphatase that translocates into mammalian cells and targets focal adhesions. EMBO J. **16:**2730–2744.
5. **Black, D. S., and J. B. Bliska.** 2000. The RhoGAP activity of the *Yersinia pseudotuberculosis* cytotoxin YopE is required for antiphagocytic function and virulence. Mol. Microbiol. **37:**515–527.
6. **Buchrieser, C., P. Glaser, C. Rusniok, H. Nedjari, H. D'Hauteville, F. Kunst, P. Sansonetti, and C. Parsot.** 2000. The virulence plasmid pWR100 and the repertoire of proteins secreted by the type III secretion apparatus of *Shigella flexneri*. Mol. Microbiol. **38:**760–771.
7. **Chen, Y., M. R. Smith, K. Thirumalai, and A. Zychlinsky.** 1996. A bacterial invasin induces macrophage apoptosis by binding directly to ICE. EMBO J. **15:**3853–3860.
8. **Datsenko, K. A., and B. L. Wanner.** 2000. One-step inactivation of chromosomal genes in *Escherichia coli* K-12 with PCR products. Proc. Natl. Acad. Sci. USA **97:**6640–6645.
9. **Demers, B., P. J. Sansonetti, and C. Parsot.** 1998. Induction of type III secretion in *Shigella flexneri* is associated with differential control of transcription of genes encoding secreted proteins. EMBO J. **17:**2894–2903.
10. **Fernandez-Prada, C. M., D. L. Hoover, B. D. Tall, A. B. Hartman, J. Kopelowitz, and M. M. Venkatesan.** 2000. *Shigella flexneri* IpaH$_{7.8}$ facilitates escape of virulent bacteria from the endocytic vacuoles of mouse and human macrophages. Infect. Immun. **68:**3608–3619.
11. **Fu, Y., and J. E. Galan.** 1999. A salmonella protein antagonizes Rac-1 and Cdc42 to mediate host-cell recovery after bacterial invasion. Nature **401:**293–297.
12. **Hardt, W. D., L. M. Chen, K. E. Schuebel, X. R. Bustelo, and J. E. Galan.** 1998. *S. typhimurium* encodes an activator of Rho GTPases that induces membrane ruffling and nuclear responses in host cells. Cell **93:**815–826.
13. **Hashimoto-Gotoh, T., M. Yamaguchi, K. Yasojima, A. Tsujimura, Y. Wakabayashi, and Y. Watanabe.** 2000. A set of temperature sensitive replication/segregation and temperature resistant plasmid vectors with different copy numbers and in an isogenic background (chloramphenicol, kanamycin, lacZ, repA, par, polA). Gene **241:**185–191.
14. **Hayashi, T., K. Makino, M. Ohnishi, K. Kurokawa, K. Ishii, K. Yokoyama, C. G. Han, E. Ohtsubo, K. Nakayama, T. Murata, M. Tanaka, T. Tobe, T. Iida, H. Takami, T. Honda, C. Sasakawa, N. Ogasawara, T. Yasunaga, S. Kuhara, T. Shiba, M. Hattori, and H. Shinagawa.** 2001. Complete genome sequence of enterohemorrhagic *Escherichia coli* O157:H7 and genomic comparison with a laboratory strain K-12. DNA Res. **8:**11–22.
15. **Heath, J. P., and G. A. Dunn.** 1978. Cell to substratum contacts of chick fibroblasts and their relation to the microfilament system. A correlated interference-reflexion and high-voltage electron-microscope study. J. Cell Sci. **29:**197–212.

16. **Ivanov, M. I., J. A. Stuckey, H. L. Schubert, M. A. Saper, and J. B. Bliska.** 2005. Two substrate-targeting sites in the *Yersinia* protein tyrosine phosphatase co-operate to promote bacterial virulence. Mol. Microbiol. **55:**1346–1356.
17. **Kadurugamuwa, J. L., M. Rohde, J. Wehland, and K. N. Timmis.** 1991. Intercellular spread of *Shigella flexneri* through a monolayer mediated by membranous protrusions and associated with reorganization of the cytoskeletal protein vinculin. Infect. Immun. **59:**3463–3471.
18. **Kane, C. D., R. Schuch, W. A. Day, and A. T. Maurelli.** 2002. MxiE regulates intracellular expression of factors secreted by the *Shigella flexneri* 2a type III secretion system. J. Bacteriol. **184:**4409–4419.
19. **Kato, J., K. Ito, A. Nakamura, and H. Watanabe.** 1989. Cloning of regions required for contact hemolysis and entry into LLC-MK2 cells from *Shigella sonnei* form I plasmid: *virF* is a positive regulator gene for these phenotypes. Infect. Immun. **57:**1391–1398.
20. **Kim, D. W., G. Lenzen, A. L. Page, P. Legrain, P. J. Sansonetti, and C. Parsot.** 2005. The *Shigella flexneri* effector OspG interferes with innate immune responses by targeting ubiquitin-conjugating enzymes. Proc. Natl. Acad. Sci. USA **102:**14046–14051.
21. **LaBrec, E. H., H. Schneider, T. J. Magnani, and S. B. Formal.** 1964. Epithelial cell penetration as an essential step in the pathogenesis of bacillary dysentery. J. Bacteriol. **88:**1503–1518.
22. **Laemmli, U. K.** 1970. Cleavage of structural proteins during the assembly of the head of bacteriophage T4. Nature **227:**680–685.
23. **Le Gall, T., M. Mavris, M. C. Martino, M. L. Bernardini, E. Denamur, and C. Parsot.** 2005. Analysis of virulence plasmid gene expression defines three classes of effectors in the type III secretion system of *Shigella flexneri*. Microbiology **151:**951–962.
24. **Lett, M. C., C. Sasakawa, N. Okada, T. Sakai, S. Makino, M. Yamada, K. Komatsu, and M. Yoshikawa.** 1989. *virG*, a plasmid-coded virulence gene of *Shigella flexneri*: identification of the *virG* protein and determination of the complete coding sequence. J. Bacteriol. **171:**353–359.
25. **Makino, S., C. Sasakawa, K. Kamata, T. Kurata, and M. Yoshikawa.** 1986. A genetic determinant required for continuous reinfection of adjacent cells on large plasmid in *S. flexneri* 2a. Cell **46:**551–555.
26. **Mavris, M., A. L. Page, R. Tournebize, B. Demers, P. Sansonetti, and C. Parsot.** 2002. Regulation of transcription by the activity of the *Shigella flexneri* type III secretion apparatus. Mol. Microbiol. **43:**1543–1553.
27. **Mavris, M., P. J. Sansonetti, and C. Parsot.** 2002. Identification of the *cis*-acting site involved in activation of promoters regulated by activity of the type III secretion apparatus in *Shigella flexneri*. J. Bacteriol. **184:**6751–6759.
28. **McGahon, A. J., S. J. Martin, R. P. Bissonnette, A. Mahboubi, Y. Shi, R. J. Mogil, W. K. Nishioka, and D. R. Green.** 1995. The end of the (cell) line: methods for the study of apoptosis *in vitro*. Methods Cell Biol. **46:**153–185.
29. **Menard, R., P. Sansonetti, and C. Parsot.** 1994. The secretion of the *Shigella flexneri* Ipa invasins is activated by epithelial cells and controlled by IpaB and IpaD. EMBO J. **13:**5293–5302.
30. **Mitobe, J., E. Arakawa, and H. Watanabe.** 2005. A sensor of the two-component system CpxA affects expression of the type III secretion system through posttranscriptional processing of InvE. J. Bacteriol. **187:**107–113.
31. **Müller, A., D. Gunther, F. Dux, M. Naumann, T. F. Meyer, and T. Rudel.** 1999. Neisserial porin (PorB) causes rapid calcium influx in target cells and induces apoptosis by the activation of cysteine proteases. EMBO J. **18:**339–352.
32. **Oaks, E. V., M. E. Wingfield, and S. B. Formal.** 1985. Plaque formation by virulent *Shigella flexneri*. Infect. Immun. **48:**124–129.
33. **Ogawa, M., T. Yoshimori, T. Suzuki, H. Sagara, N. Mizushima, and C. Sasakawa.** 2005. Escape of intracellular *Shigella* from autophagy. Science **307:**727–731.
34. **Okuda, J., T. Toyotome, N. Kataoka, M. Ohno, H. Abe, Y. Shimura, A. Seyedarabi, R. Pickersgill, and C. Sasakawa.** 2005. *Shigella* effector IpaH9.8 binds to a splicing factor U2AF(35) to modulate host immune responses. Biochem. Biophys. Res. Commun. **333:**531–539.
35. **Orita, Y., K. Nishizaki, J. Sasaki, S. Kanda, N. Kimura, S. Nomiya, K. Yuen, and Y. Masuda.** 1999. Does TUNEL staining during peri- and post-natal development of the mouse inner ear indicate apoptosis? Acta Otolaryngol. Suppl. **540:**22–26.
36. **Pal, T., J. W. Newland, B. D. Tall, S. B. Formal, and T. L. Hale.** 1989. Intracellular spread of *Shigella flexneri* associated with the *kcpA* locus and a 140-kilodalton protein. Infect. Immun. **57:**477–486.
37. **Parsot, C., E. Ageron, C. Penno, M. Mavris, K. Jamoussi, H. d'Hauteville, P. Sansonetti, and B. Demers.** 2005. A secreted anti-activator, OspD1, and its chaperone, Spa15, are involved in the control of transcription by the type III secretion apparatus activity in *Shigella flexneri*. Mol. Microbiol. **56:**1627–1635.
38. **Parsot, C., R. Menard, P. Gounon, and P. J. Sansonetti.** 1995. Enhanced secretion through the *Shigella flexneri* Mxi-Spa translocon leads to assembly of extracellular proteins into macromolecular structures. Mol. Microbiol. **16:**291–300.
39. **Parsot, C., and P. J. Sansonetti.** 1999. The virulence plasmid of shigellae: an archipelago of pathogenicity islands? p. 151–165. *In* J. B. Kaper and J. Kacker (ed.), Pathogenicity islands and other mobile virulence elements. American Society for Microbiology, Washington, D.C.
40. **Prevost, M. C., M. Lesourd, M. Arpin, F. Vernel, J. Mounier, R. Hellio, and P. J. Sansonetti.** 1992. Unipolar reorganization of F-actin layer at bacterial division and bundling of actin filaments by plastin correlate with movement of *Shigella flexneri* within HeLa cells. Infect. Immun. **60:**4088–4099.
41. **Pridmore, R. D.** 1987. New and versatile cloning vectors with kanamycin-resistance marker. Gene **56:**309–312.
42. **Rosqvist, R., A. Forsberg, and H. Wolf-Watz.** 1991. Intracellular targeting of the *Yersinia* YopE cytotoxin in mammalian cells induces actin microfilament disruption. Infect. Immun. **59:**4562–4569.
43. **Sansonetti, P. J., D. J. Kopecko, and S. B. Formal.** 1982. Involvement of a large plasmid in the invasive ability of *Shigella flexneri*. Infect. Immun. **35:**852–860.
44. **Sansonetti, P. J., A. Ryter, P. Clerc, A. T. Maurelli, and J. Mounier.** 1986. Multiplication of *Shigella flexneri* within HeLa cells: lysis of the phagocytic vacuole and plasmid-mediated contact hemolysis. Infect. Immun. **51:**461–469.
45. **Schuch, R., and A. T. Maurelli.** 1999. The Mxi-Spa type III secretory pathway of *Shigella flexneri* requires an outer membrane lipoprotein, MxiM, for invasin translocation. Infect. Immun. **67:**1982–1991.
46. **Shaikh, N., J. Terajima, and H. Watanabe.** 2003. IpaC of *Shigella* binds to the C-terminal domain of β-catenin. Microb. Pathog. **35:**107–117.
47. **Studier, F. W., A. H. Rosenberg, J. J. Dunn, and J. W. Dubendorff.** 1990. Use of T7 RNA polymerase to direct expression of cloned genes. Methods Enzymol. **185:**60–89.
48. **Tamano, K., S. Aizawa, E. Katayama, T. Nonaka, S. Imajoh-Ohmi, A. Kuwae, S. Nagai, and C. Sasakawa.** 2000. Supramolecular structure of the *Shigella* type III secretion machinery: the needle part is changeable in length and essential for delivery of effectors. EMBO J. **19:**3876–3887.
49. **Terajima, J., E. Moriishi, T. Kurata, and H. Watanabe.** 1999. Preincubation of recombinant Ipa proteins of *Shigella sonnei* promotes entry of non-invasive *Escherichia coli* into HeLa cells. Microb. Pathog. **26:**223–230.
50. **Toyotome, T., T. Suzuki, A. Kuwae, T. Nonaka, H. Fukuda, S. Imajoh-Ohmi, T. Toyofuku, M. Hori, and C. Sasakawa.** 2001. *Shigella* protein IpaH(9.8) is secreted from bacteria within mammalian cells and transported to the nucleus. J. Biol. Chem. **276:**32071–32079.
51. **Tran Van Nhieu, G., E. Caron, A. Hall, and P. J. Sansonetti.** 1999. IpaC induces actin polymerization and filopodia formation during *Shigella* entry into epithelial cells. EMBO J. **18:**3249–3262.
52. **Tu, Y., S. Wu, X. Shi, K. Chen, and C. Wu.** 2003. Migfilin and Mig-2 link focal adhesions to filamin and the actin cytoskeleton and function in cell shape modulation. Cell **113:**37–47.
53. **Uchiya, K., T. Tobe, K. Komatsu, T. Suzuki, M. Watarai, I. Fukuda, M. Yoshikawa, and C. Sasakawa.** 1995. Identification of a novel virulence gene, virA, on the large plasmid of *Shigella*, involved in invasion and intercellular spreading. Mol. Microbiol. **17:**241–250.
54. **Watanabe, H., E. Arakawa, K.-I. Ito, J.-I. Kato, and A. Nakamura.** 1990. Genetic analysis of an invasion region by use of a Tn*3-lac* transposon and identification of a second positive regulator gene, *invE*, for cell invasion of *Shigella sonnei*: significant homology of InvE with ParB of plasmid P1. J. Bacteriol. **172:**619–629.
55. **Watanabe, H., and A. Nakamura.** 1985. Large plasmids associated with virulence in *Shigella* species have a common function necessary for epithelial cell penetration. Infect. Immun. **48:**260–262.
56. **Watanabe, H., and A. Nakamura.** 1986. Identification of *Shigella sonnei* form I plasmid genes necessary for cell invasion and their conservation among *Shigella* species and enteroinvasive *Escherichia coli*. Infect. Immun. **53:**352–358.
57. **Yanisch-Perron, C., J. Vieira, and J. Messing.** 1985. Improved M13 phage cloning vectors and host strains: nucleotide sequences of the M13mp18 and pUC19 vectors. Gene **33:**103–120.
58. **Yoshida, S., E. Katayama, A. Kuwae, H. Mimuro, T. Suzuki, and C. Sasakawa.** 2002. *Shigella* deliver an effector protein to trigger host microtubule destabilization, which promotes Rac1 activity and efficient bacterial internalization. EMBO J. **21:**2923–2935.
59. **Zychlinsky, A., M. C. Prevost, and P. J. Sansonetti.** 1992. *Shigella flexneri* induces apoptosis in infected macrophages. Nature **358:**167–169.

Editor: J. B. Bliska